Open Access

Journal of Radiology and Oncology

Heighten Science
PUBLICATIONS Corporation
ISSN
2573-7724

Research Article

Empirical formulae for calculating γ-ray detectors effective solid angle ratio

Ahmed M El Khatib[1], Mohamed S Badawi[1,2]*, Mohamed A Elzaher[3], Mona M Gouda[1], Abouzeid A Thabet[4], Mahmoud I Abbas[1] and Kholud S Almugren[5]

[1]Physics Department, Faculty of Science, Alexandria University, 21511 Alexandria, Egypt
[2]Department of Physics, Faculty of Science, Beirut Arab University, Beirut, Lebanon
[3]Department of Basic and Applied Sciences, Faculty of Engineering, Arab Academy for Science, Technology and Maritime Transport, Alexandria, Egypt
[4]Department of Medical Equipment Technology, Faculty of Allied Medical Sciences, Pharos University in Alexandria, Alexandria, Egypt
[5]Physics Department, Faculty of Science, Princess Nourah Bint Abdulrahaman University, 11544-55532 Riyadh, Saudi Arabia

***Address for Correspondence:** Mohamed S Badawi, Physics Department, Faculty of Science, Alexandria University, 21511 Alexandria, Egypt, Tel: +201005154976; Email: ms241178@hotmail.com

Submitted: 19 December 2016
Approved: 25 January 2017
Published: 27 January 2017

Keywords: NaI (Tl) detector; Effective solid angle ratio; Full-Energy peak efficiency

Acknowledgement: All of us would like to thank Prof. Dr. Nasser. M El Maghraby, Dean of Basic and Applied Science Institute, Arab Academy for Science, Technology and Maritime Transport, Alexandria, Egypt for his valuable assistance in the mathematical part.

ABSTRACT

Determination of the detector efficiency using volumetric cylindrical sources is very important in various scientific and industrial fields, especially in the field of quantitative analysis. To calculate the absolute activity of any sample, the full-energy peak efficiency (FEPE) of the detector is needed. By applying the efficiency transfer method, the FEPE of the detector would be determined easily without using the standard sources. This approach depends on two main factors. The first one, is the reference efficiency of the reference source, which is determined experimentally, and the second one, is the calculation of the effective solid angle ratio between the sample and the reference source geometries. This work introduces an empirical formula for calculating the second factor for using two different sizes of NaI(Tl) detectors. The validity of this empirical formula was successfully demonstrated by comparing the calculating values with the experimental values.

INTRODUCTION

The scintillation counters are used to measure the radiation in different applications such as, radiation survey meters, medical imaging, nuclear plant safety, measuring radon levels, oil well logging and monitoring for radioactive contamination. In the gamma-ray spectroscopy, one usually needs to know the full-energy peak efficiency for any specific source-to-detector configuration of concern. Traditionally, measurements are performed in gamma-ray spectrometry by the relative method, according to which the measured sample is first prepared, that should match the used standard source in all the important characteristics, such as its size, chemical composition and density [1]. This method is tedious and time consuming process. In order to overcome the problems of the experimental method, several non-experimental methods [2-6] have been proposed and applied, depending on the photon energy, source-to-detector geometry and volume. One of the most common approaches is called the efficiency transfer method. In this technique, the detector efficiency of using various source dimensions is derived from the known efficiency for the reference source-to-detector geometry. The efficiency transfer method is particularly useful due to, its insensitivity to the

How to cite this article: El Khatib AM, Badawi MS, Elzaher MA, Gouda MM, Thabet AA, et al. Empirical Formulae for Calculating γ-ray Detectors Effective Solid Angle Ratio. J Radiol Oncol. 2017; 1: 012-021. https://doi.org/10.29328/journal.jro.1001002

inaccuracy of the input data, such as the uncertainty of the detector characterization [7,8].

Badawi, et al. [9-11] were introduced an approach to calculate the full-energy peak efficiency for NaI(Tl) and HPGe detectors, with respect to different volumetric sources. This approach stated that, the detector efficiency using a certain cylindrical radioactive source, $\varepsilon\left(E,Cyl\right)$, equal the reference efficiency of using reference radioactive point source, $\varepsilon\left(E,P_i\right)$, with the same detector multiplied by the effective solid angle ratio, R, between the two geometries and expressed by the following equation

$$\varepsilon\left(E,Cyl\right)=\varepsilon\left(E,P_i\right).R \tag{1}$$

Calculations of the effective solid angle are based on the direct mathematical method which reported by Selim and Abbas [12-16] and used successfully before to calibrate different detectors with different sources. The present work will introduce empirical equations to calculate the effective solid angle ratios of two NaI(Tl) detectors with different geometries. The effective solid angle ratio can be used as a conversion factor from using the radioactive point source case to the case in which the cylindrical radioactive sources were used. Consequently, the corresponding full-energy peak efficiency can be calculated simply.

EXPERIMENTAL SETUP

The full-energy peak efficiency (FEPE) values were determined for two NaI (Tl) detectors with resolutions 8.5% and 7.5% at the 662 keV peaks of ^{137}Cs labeled as D1 and D2 respectively. The manufacturer parameters and the setup values are shown in table 1. The experimental measurements were carried out by using point and cylindrical radioactive sources.

The radioactive standard point sources (^{241}Am, ^{133}Ba, ^{152}Eu, ^{137}Cs, and ^{60}Co) are used for the calibration of gamma spectrometers. The radioactive substance is a very thin, compact grained layer applied to a circular area about 5 mm in diameter, in the middle of the source between two polyethylene foils and each having a mass per unit area of (21.3±1.8) mg.cm^{-2}. By heating under pressure, the two foils are welded together over the whole area so that they are leak-proofed. To facilitate handling, the foil 26 mm in diameter is mounted in a circular aluminum ring (outer diameter: 30 mm, height: 3 mm) from which it can easily be removed if and when required. These point sources were purchased from the Physikalisch-Technische Bundesanstalt (PTB) in Braunschweig and Berlin, which is the national institute for science and technology and the highest technical authority of the Federal Republic of Germany in the field of metrology and certain sectors of safety engineering. The sources activities and their uncertainties, half-lives, photon energies, and photon emission probabilities per decay for all of PTB sources are listed in table 2.

The homemade Plexiglas holder was used to measure these standard point sources, each at seven different axial distances starting from 20 cm up to 50 cm from the surface of the detector (with a 5 cm as a step). The measurements started from a source-to-detector distance equals 20 cm to minimize the effect of the coincidence summing effect. Spectra were recorded as, P4D1, where P refers to the source type (point) measured at the detector (D1) at position number (4), which equal 20 cm.

The cylindrical radioactive sources were in polypropylene plastic vials form with radius greater than the radius of the detectors, and volumes of 200 ml, 300 ml and 400 ml filled with an aqueous solution containing ^{152}Eu radionuclide, which used for the calibration process. The ^{152}Eu source emits γ-ray in the energy range from 121.78 keV up to 1408.01 keV. Table 3 shows the source dimensions. In order to minimize the dead

Table 1: The manufacturer parameters and the setup values.

Items	Detector (D1)	Detector (D2)
Manufacturer	Canberra	Canberra
Serial Number	09L 654	09L 652
Detector Model	802	802
Type	Cylindrical	Cylindrical
Mounting	Vertical	Vertical
Resolution (FWHM) at 661 keV	7.5%	8.5%
Cathode to Anode voltage	+900 V dc	+800V dc
Dynode to Dynode	+80 V dc	+80 V dc
Cathode to Dynode	+150 V dc	+150 V dc
Tube Base	Model 2007	Model 2007
Shaping Mode	Gaussian	Gaussian
Detector Type	NaI(Tl)	NaI(Tl)
Crystal Diameter (mm)	50.8	76.2
Crystal Length (mm)	50.8	76.2
Top cover Thickness (mm)	Al (0.5)	Al (0.5)
Side cover Thickness (mm)	Al (0.5)	Al (0.5)
Reflector – Oxide (mm)	2.5	2.5
Weight (Kg)	0.77	1.8
Outer Diameter (mm)	57.2	80.9
Outer Length (mm)	53.9	79.4
Crystal Volume in (cm^3)	103.004	347.639

Table 2: Point sources activities and their uncertainties, half lives, photon energies and photon emission probabilities per decay for the all radionuclides used in this work.

PTB Nuclide	Energy (keV)	Emission Probability %	Half Life (Days)	Activity (kBq) At 1.June 2009 00:00 Hr	Uncertainty (KBq)
^{241}Am	59.52	35.9	157861.05	259.0	±2.6
^{133}Ba	80.99	34.1	3847.91	275.3	±2.8
^{152}Eu	121.78	28.4	4943.29	290.0	±4.0
	244.69	7.49			
	344.28	26.6			
	778.91	12.96			
	964.13	14.0			
	1408.01	20.87			
^{137}Cs	661.66	85.21	11004.98	385.0	±4.0
^{60}Co	1173.23	99.99	1925.31	212.1	±1.5
	1332.51	99.98			

Table 3: Parameters of the radioactive cylindrical volumetric sources.

Items	Source Volume (ml)		
	V1=200	V2=300	V3=400
Inner diameter (mm)	111.50		
Height (mm)	21.45	31.59	41.83
Wall and Bottom thickness (mm)	2.03		
Activity (Bq) At 1.Jan 2010 00:00 Hr	5048 ± 49.98		

time, the activity of the sources is prepared to be a few kilo Becquerel (5048±49.98 Bq).

The radioactive volumetric cylindrical sources were measured on a 0.36 cm thickness Plexiglas cover and placed directly on the detector end-cap. These measurements were done using two cylindrical detectors with numbers (D1 & D2). Figure 1 shows a diagram

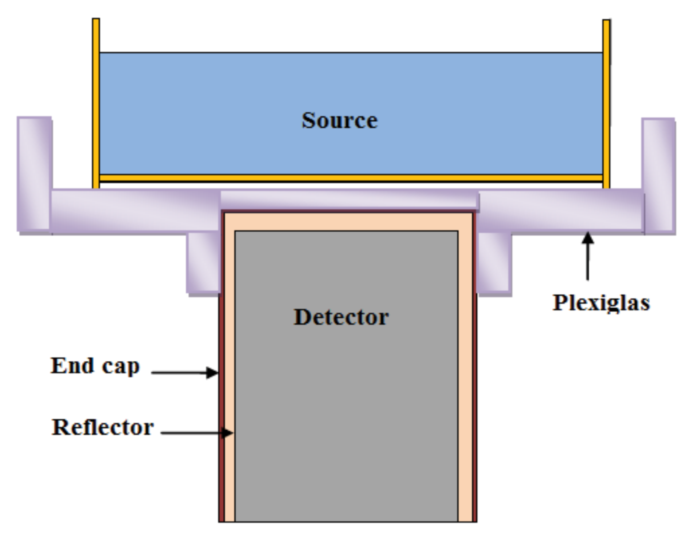

Figure 1: A diagram of a cylindrical detector with radioactive cylindrical source.

of a cylindrical detector with cylindrical source. Spectra were recorded as V1D2, where V1 is the volume (V1) measured at the detector (D2). The angular correlation effects can be neglected for the low source-to-detector distance [17,18].

All the measurements are carried out to obtain statistically significant main peaks in the spectra that are recorded and processed by winTMCA32 software made by ICx Technologies. Measured spectrum, which saved as spectrum ORTEC files can be opened by the Genie 2000 data acquisition and analysis software made by Canberra. The acquisition time is high enough to get at least the number of counts 20,000, which make the statistical uncertainties less than 0.1%. The spectra are analyzed with the program using its automatic peak search and peak area calculations, along with changes in the peak fit using the interactive peak fit interface when necessary to reduce the residuals and error in the peak area values. The peak areas, the live time, the run time and the start time for each spectrum were entered in the spreadsheets that are used to perform the calculations necessary to generate the efficiency curves.

RESULTS AND DISCUSSIONS

The efficiency transfer theoretical method (ETTM) has been used to convert the (FEPE) curve for using radioactive point source at positions start from P4 up to P10 to the (FEPE) for using radioactive cylindrical sources, which represented in V1, V2, and V3. These calculations extended for two cylindrical NaI(Tl) detectors (D1 & D2). By using equation (1) and the experimental efficiency values for using point and cylindrical radioactive sources, that published before in 2012 [19], the one can calculate the effective solid angle ratio, R, values for both detectors experimentally as tabulated in table 4.

The analytical expressions presented in [19] were used to calculate the effective solid angle ratio as presented in table 5, these values were tested before to obtain the detector FEPE and it was accepted by comparison with the experimental values. The percentage deviations between the effective solid angle ratio values obtained by the two methods are shown in figure 2. A remarkable agreement between them was achieved with discrepancies less than 10%.

By plotting a three dimensional relation between the Log values of the point source position, P (cm), the effective solid angle ratio, R, and the photon energy, E (keV) for the two detectors (D1 & D2) was done as shown in figure 3. The plotted data for each

Table 4: The values of the effective solid angle ratio, R, for both detectors, which were obtained experimentally.

Effective solid angle ratio between different volumes and different positions with respect to (D1 and D2).(From Experimental Data)															
		Detector (D1) Effective solid angle ratio							Detector (D2) Effective solid angle ratio						
Nuclide	**Energy**	$\frac{\Omega_{V1}}{\Omega_{P4}}$	$\frac{\Omega_{V1}}{\Omega_{P5}}$	$\frac{\Omega_{V1}}{\Omega_{P6}}$	$\frac{\Omega_{V1}}{\Omega_{P7}}$	$\frac{\Omega_{V1}}{\Omega_{P8}}$	$\frac{\Omega_{V1}}{\Omega_{P9}}$	$\frac{\Omega_{V1}}{\Omega_{P10}}$	$\frac{\Omega_{V1}}{\Omega_{P4}}$	$\frac{\Omega_{V1}}{\Omega_{P5}}$	$\frac{\Omega_{V1}}{\Omega_{P6}}$	$\frac{\Omega_{V1}}{\Omega_{P7}}$	$\frac{\Omega_{V1}}{\Omega_{P8}}$	$\frac{\Omega_{V1}}{\Omega_{P9}}$	$\frac{\Omega_{V1}}{\Omega_{P10}}$
Eu-152	121.78	15.722	23.735	32.957	44.330	58.034	72.859	89.042	11.984	17.753	25.185	33.687	44.037	54.425	66.609
Eu-152	244.69	15.795	23.603	33.259	44.087	57.531	72.710	87.406	12.380	18.381	25.950	34.453	45.196	55.989	68.073
Eu-152	344.28	15.850	23.578	33.370	44.110	57.503	73.168	87.516	12.572	18.519	26.253	34.492	45.250	56.562	68.579
Eu-152	778.9	16.165	24.068	34.135	45.149	58.498	74.488	89.140	12.935	19.337	26.901	35.421	45.992	57.317	70.413
Eu-152	964.13	16.298	24.132	34.285	45.482	58.722	74.473	89.618	13.070	19.444	27.349	35.753	46.408	57.349	70.154
Eu-152	1408.01	16.465	24.458	34.752	45.831	59.643	74.802	89.715	13.182	19.596	27.499	36.195	46.989	58.306	71.399
Nuclide	**Energy**	$\frac{\Omega_{V2}}{\Omega_{P4}}$	$\frac{\Omega_{V2}}{\Omega_{P5}}$	$\frac{\Omega_{V2}}{\Omega_{P6}}$	$\frac{\Omega_{V2}}{\Omega_{P7}}$	$\frac{\Omega_{V2}}{\Omega_{P8}}$	$\frac{\Omega_{V2}}{\Omega_{P9}}$	$\frac{\Omega_{V2}}{\Omega_{P10}}$	$\frac{\Omega_{V2}}{\Omega_{P4}}$	$\frac{\Omega_{V2}}{\Omega_{P5}}$	$\frac{\Omega_{V2}}{\Omega_{P6}}$	$\frac{\Omega_{V2}}{\Omega_{P7}}$	$\frac{\Omega_{V2}}{\Omega_{P8}}$	$\frac{\Omega_{V2}}{\Omega_{P9}}$	$\frac{\Omega_{V2}}{\Omega_{P10}}$
Eu-152	121.78	13.216	19.951	27.703	37.263	48.782	61.244	74.847	10.313	15.278	21.674	28.990	37.897	46.837	57.322
Eu-152	244.69	13.222	19.758	27.841	36.905	48.159	60.864	73.166	10.572	15.697	22.161	29.423	38.598	47.815	58.134
Eu-152	344.28	13.372	19.892	28.153	37.214	48.514	61.730	73.835	10.679	15.731	22.300	29.298	38.437	48.045	58.253
Eu-152	778.9	13.755	20.480	29.046	38.418	49.777	63.383	75.851	11.215	16.767	23.326	30.713	39.878	49.699	61.054
Eu-152	964.13	13.911	20.597	29.263	38.820	50.121	63.565	76.491	11.303	16.814	23.650	30.918	40.132	49.593	60.666
Eu-152	1408.01	14.095	20.938	29.749	39.234	51.058	64.035	76.802	11.435	16.999	23.855	31.398	40.761	50.579	61.937
Nuclide	**Energy**	$\frac{\Omega_{V3}}{\Omega_{P4}}$	$\frac{\Omega_{V3}}{\Omega_{P5}}$	$\frac{\Omega_{V3}}{\Omega_{P6}}$	$\frac{\Omega_{V3}}{\Omega_{P7}}$	$\frac{\Omega_{V3}}{\Omega_{P8}}$	$\frac{\Omega_{V3}}{\Omega_{P9}}$	$\frac{\Omega_{V3}}{\Omega_{P10}}$	$\frac{\Omega_{V3}}{\Omega_{P4}}$	$\frac{\Omega_{V3}}{\Omega_{P5}}$	$\frac{\Omega_{V3}}{\Omega_{P6}}$	$\frac{\Omega_{V3}}{\Omega_{P7}}$	$\frac{\Omega_{V3}}{\Omega_{P8}}$	$\frac{\Omega_{V3}}{\Omega_{P9}}$	$\frac{\Omega_{V3}}{\Omega_{P10}}$
Eu-152	121.78	11.152	16.835	23.377	31.444	41.164	51.679	63.158	8.760	12.977	18.410	24.624	32.190	39.783	48.690
Eu-152	244.69	11.372	16.994	23.947	31.743	41.423	52.352	62.933	9.009	13.376	18.884	25.072	32.889	40.743	49.536
Eu-152	344.28	11.483	17.082	24.176	31.957	41.661	53.010	63.405	9.167	13.504	19.143	25.150	32.995	41.243	50.005
Eu-152	778.9	11.901	17.720	25.132	33.242	43.070	54.842	65.630	9.582	14.325	19.929	26.241	34.072	42.462	52.164
Eu-152	964.13	12.024	17.803	25.294	33.553	43.321	54.942	66.115	9.878	14.695	20.669	27.021	35.073	43.342	53.020
Eu-152	1408.01	12.287	18.251	25.933	34.201	44.508	55.820	66.949	9.997	14.861	20.855	27.450	35.635	44.219	54.148

Table 5: The values of the effective solid angle ratio, R, for both detectors, which are obtained analytically [19].

Effective solid angle ratio between different volumes and different positions with respect to (D1 and D2).															
		Detector (D1) Effective solid angle ratio							Detector (D2) Effective solid angle ratio						
Nuclide	**Energy**	$\frac{\Omega_{V1}}{\Omega_{P4}}$	$\frac{\Omega_{V1}}{\Omega_{P5}}$	$\frac{\Omega_{V1}}{\Omega_{P6}}$	$\frac{\Omega_{V1}}{\Omega_{P7}}$	$\frac{\Omega_{V1}}{\Omega_{P8}}$	$\frac{\Omega_{V1}}{\Omega_{P9}}$	$\frac{\Omega_{V1}}{\Omega_{P10}}$	$\frac{\Omega_{V1}}{\Omega_{P4}}$	$\frac{\Omega_{V1}}{\Omega_{P5}}$	$\frac{\Omega_{V1}}{\Omega_{P6}}$	$\frac{\Omega_{V1}}{\Omega_{P7}}$	$\frac{\Omega_{V1}}{\Omega_{P8}}$	$\frac{\Omega_{V1}}{\Omega_{P9}}$	$\frac{\Omega_{V1}}{\Omega_{P10}}$
Am-241	59.53	14.637	21.861	31.549	40.638	53.398	66.338	83.377	11.666	17.293	24.512	32.344	42.805	51.785	62.635
Ba-133	80.99	14.903	22.260	31.895	41.453	54.488	68.058	84.158	11.703	17.359	24.550	32.436	42.850	52.310	63.409
Eu-152	121.78	15.209	22.720	32.416	42.347	55.684	69.808	85.445	11.867	17.612	24.869	32.889	43.394	53.301	64.747
Eu-152	244.69	15.779	23.573	33.496	43.962	57.849	72.828	88.196	12.293	18.254	25.728	34.071	44.887	55.523	67.663
Eu-152	344.28	16.080	24.024	34.078	44.815	58.992	74.403	89.687	12.528	18.608	26.206	34.725	45.718	56.725	69.230
Cs-137	661.66	16.633	24.852	35.145	46.375	61.084	77.302	92.414	12.965	19.266	27.093	35.941	47.263	58.969	72.169
Eu-152	778.9	16.766	25.051	35.401	46.751	61.588	77.999	93.070	13.070	19.424	27.307	36.233	47.635	59.509	72.876
Eu-152	964.13	16.933	25.302	35.724	47.224	62.223	78.880	93.897	13.203	19.625	27.577	36.603	48.104	60.193	73.773
Co-60	1173.23	17.081	25.523	36.010	47.642	62.783	79.658	94.628	13.322	19.803	27.818	36.933	48.523	60.802	74.571
Co-60	1332.5	17.175	25.663	36.191	47.907	63.138	80.149	95.090	13.397	19.916	27.969	37.141	48.788	61.186	75.074
Eu-152	1408.01	17.216	25.724	36.270	48.022	63.292	80.363	95.293	13.429	19.964	28.034	37.230	48.900	61.350	75.290
Nuclide	**Energy**	$\frac{\Omega_{V2}}{\Omega_{P4}}$	$\frac{\Omega_{V2}}{\Omega_{P5}}$	$\frac{\Omega_{V2}}{\Omega_{P6}}$	$\frac{\Omega_{V2}}{\Omega_{P7}}$	$\frac{\Omega_{V2}}{\Omega_{P8}}$	$\frac{\Omega_{V2}}{\Omega_{P9}}$	$\frac{\Omega_{V2}}{\Omega_{P10}}$	$\frac{\Omega_{V2}}{\Omega_{P4}}$	$\frac{\Omega_{V2}}{\Omega_{P5}}$	$\frac{\Omega_{V2}}{\Omega_{P6}}$	$\frac{\Omega_{V2}}{\Omega_{P7}}$	$\frac{\Omega_{V2}}{\Omega_{P8}}$	$\frac{\Omega_{V2}}{\Omega_{P9}}$	$\frac{\Omega_{V2}}{\Omega_{P10}}$
Am-241	59.53	12.081	18.044	26.041	33.544	44.076	54.757	68.821	9.926	14.714	20.855	27.519	36.419	44.060	53.292
Ba-133	80.99	12.365	18.470	26.464	34.394	45.210	56.469	69.827	10.011	14.851	21.002	27.749	36.657	44.751	54.246
Eu-152	121.78	12.691	18.959	27.050	35.336	46.466	58.251	71.300	10.214	15.159	21.405	28.308	37.350	45.877	55.728
Eu-152	244.69	13.301	19.872	28.238	37.060	48.767	61.394	74.350	10.698	15.886	22.391	29.651	39.064	48.320	58.886
Eu-152	344.28	13.628	20.361	28.882	37.981	49.996	63.057	76.010	10.966	16.288	22.938	30.395	40.018	49.652	60.598

Cs-137	661.66	14.232	21.265	30.072	39.682	52.268	66.145	79.076	11.467	17.039	23.962	31.787	41.800	52.153	63.828
Eu-152	778.9	14.378	21.484	30.360	40.094	52.818	66.893	79.817	11.588	17.221	24.210	32.124	42.232	52.760	64.611
Eu-152	964.13	14.563	21.761	30.725	40.615	53.514	67.841	80.756	11.742	17.452	24.524	32.551	42.779	53.529	65.606
Co-60	1173.23	14.727	22.006	31.048	41.077	54.131	68.680	81.587	11.879	17.658	24.804	32.932	43.267	54.216	66.493
Co-60	1332.5	14.831	22.161	31.252	41.369	54.522	69.212	82.114	11.966	17.788	24.982	33.173	43.576	54.649	67.054
Eu-152	1408.01	14.877	22.229	31.342	41.497	54.693	69.445	82.346	12.003	17.844	25.058	33.277	43.709	54.837	67.297
Nuclide	**Energy**	$\frac{\Omega_{V3}}{\Omega_{P4}}$	$\frac{\Omega_{V3}}{\Omega_{P5}}$	$\frac{\Omega_{V3}}{\Omega_{P6}}$	$\frac{\Omega_{V3}}{\Omega_{P7}}$	$\frac{\Omega_{V3}}{\Omega_{P8}}$	$\frac{\Omega_{V3}}{\Omega_{P9}}$	$\frac{\Omega_{V3}}{\Omega_{P10}}$	$\frac{\Omega_{V3}}{\Omega_{P4}}$	$\frac{\Omega_{V3}}{\Omega_{P5}}$	$\frac{\Omega_{V3}}{\Omega_{P6}}$	$\frac{\Omega_{V3}}{\Omega_{P7}}$	$\frac{\Omega_{V3}}{\Omega_{P8}}$	$\frac{\Omega_{V3}}{\Omega_{P9}}$	$\frac{\Omega_{V3}}{\Omega_{P10}}$
Am-241	59.53	10.175	15.197	21.932	28.251	37.121	46.117	57.962	8.322	12.336	17.486	23.073	30.536	36.942	44.682
Ba-133	80.99	10.459	15.622	22.384	29.092	38.240	47.763	59.062	8.425	12.498	17.675	23.353	30.850	37.661	45.652
Eu-152	121.78	10.785	16.112	22.987	30.029	39.488	49.503	60.592	8.632	12.811	18.089	23.923	31.564	38.770	47.095
Eu-152	244.69	11.400	17.032	24.202	31.763	41.798	52.620	63.724	9.110	13.527	19.066	25.249	33.264	41.145	50.142
Eu-152	344.28	11.733	17.529	24.865	32.699	43.043	54.288	65.440	9.375	13.925	19.611	25.986	34.212	42.449	51.807
Cs-137	661.66	12.354	18.458	26.103	34.444	45.369	57.414	68.638	9.874	14.673	20.635	27.373	35.996	44.911	54.964
Eu-152	778.9	12.505	18.684	26.404	34.870	45.936	58.177	69.417	9.996	14.855	20.884	27.711	36.430	45.512	55.734
Eu-152	964.13	12.697	18.972	26.787	35.410	46.656	59.146	70.406	10.151	15.087	21.201	28.140	36.982	46.276	56.716
Co-60	1173.23	12.868	19.227	27.127	35.890	47.296	60.008	71.285	10.289	15.294	21.484	28.524	37.475	46.958	57.592
Co-60	1332.5	12.976	19.389	27.343	36.195	47.702	60.554	71.842	10.376	15.425	21.663	28.767	37.788	47.390	58.147
Eu-152	1408.01	13.024	19.461	27.438	36.329	47.881	60.795	72.089	10.414	15.482	21.741	28.872	37.923	47.578	58.388

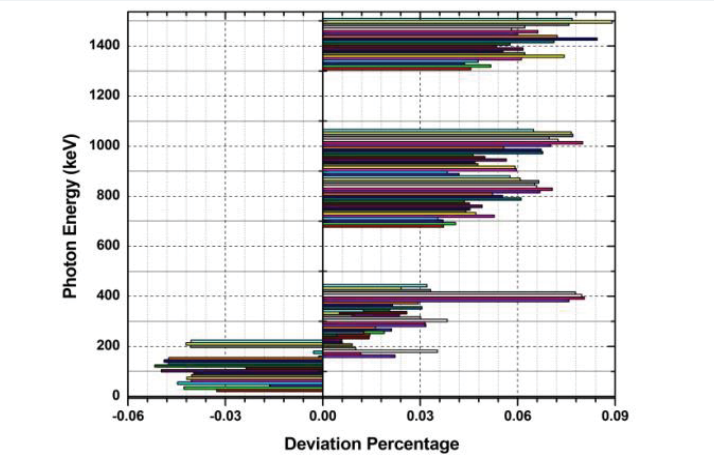

Figure 2a: The deviation between the calculated effective solid angle ratio, R, that obtained analytically and the experimental one for D1.

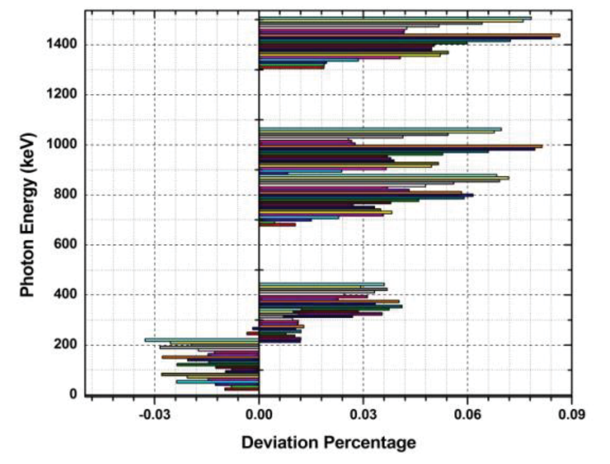

Figure 2b: The deviation between the calculated effective solid angle ratio, R, that obtained analytically and the experimental one for D2.

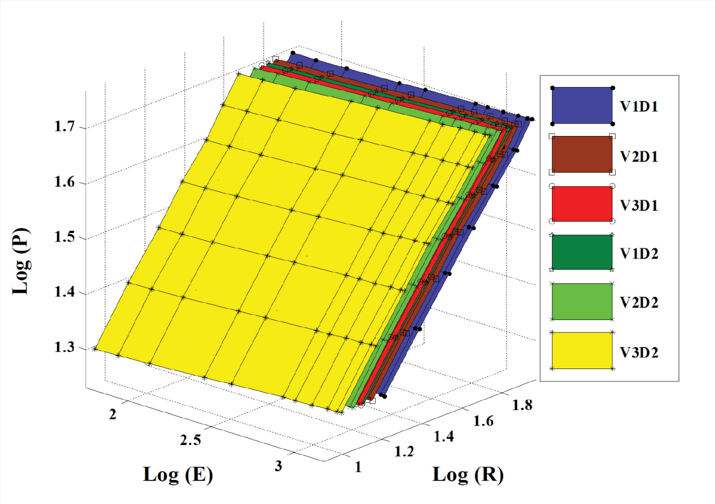

Figure 3: The relation between Log values of radioactive point source positions, P, solid angle ratio, R, and the photon energy, E, for D1 and D2.

source volume (ml) with the two detectors have shown semi plane shape and the empirical formulae that represent these shapes are described below to calculate the effective solid angle ratios, R, for both detectors.

The empirical formula for the detector (D1) is given by:

$$\mathrm{Log}(E) - 26.77\,\mathrm{Log}(R) + 49.18\,\mathrm{Log}(P) - 0.0176\,V - 30.62 = 0 \qquad (2)$$

while, the empirical formula for the detector (D2) is given by:

$$\mathrm{Log}(E) - 26.77\,\mathrm{Log}(R) + 49.18\,\mathrm{Log}(P) - 0.0166\,V - 33.63 = 0 \qquad (3)$$

By knowing the photon energy and the reference position, the effective solid angle ratio, R, for both detectors was calculated using equations (2) and (3). The obtained values were tabulated in table 6. Therefore, these equations provide a simple method to calculate the full-energy peak efficiency (FEPE) of two different cylindrical NaI(Tl) scintillation detectors. These two formulae are valid through a wide energy range and different radioactive volumetric source geometries. The percentage deviations between the calculated effective solid angle ratio, that obtained experimentally and that obtained from equations (2) and (3) were shown in figure 4. A remarkable agreement between them was achieved with discrepancies less than 7%.

The main advantage of this process is the simplicity of obtaining the effective solid angle ratios, R, especially in between any two measured positions, without using analytical or experimental calculations. These ratios are considered to be the efficiency conversion factor between any two different geometrical conditions, and used to save the time in absent the standard calibration sources.

CONCLUSIONS

The present work leads to a simplified method to calculate the effective solid angle ratio empirical, which can be used to calculate the conversion factors of the detector efficiency, in the case of using point and cylindrical radioactive sources. The efficiencies can be determined at any calibration position or any energy situated in the domain of the study based on these conversion factors. These formulas are valid through a wide energy range and different source-to-detector geometries. Therefore the corresponding full-energy peak efficiency can be calculated simply, and the activity of unknown samples measured in the same conditions can be determined easily.

Table 6: The values of the effective solid angle ratio, R, for both detectors, which are obtained from empirical equations.

Effective solid angle ratio between different volumes and different positions with respect to (D1 and D2).(from the empirical formula)															
		Detector (D1) Effective solid angle ratio							Detector (D2) Effective solid angle ratio						
Nuclide	**Energy**	$\frac{\Omega_{V1}}{\Omega_{P4}}$	$\frac{\Omega_{V1}}{\Omega_{P5}}$	$\frac{\Omega_{V1}}{\Omega_{P6}}$	$\frac{\Omega_{V1}}{\Omega_{P7}}$	$\frac{\Omega_{V1}}{\Omega_{P8}}$	$\frac{\Omega_{V1}}{\Omega_{P9}}$	$\frac{\Omega_{V1}}{\Omega_{P10}}$	$\frac{\Omega_{V1}}{\Omega_{P4}}$	$\frac{\Omega_{V1}}{\Omega_{P5}}$	$\frac{\Omega_{V1}}{\Omega_{P6}}$	$\frac{\Omega_{V1}}{\Omega_{P7}}$	$\frac{\Omega_{V1}}{\Omega_{P8}}$	$\frac{\Omega_{V1}}{\Omega_{P9}}$	$\frac{\Omega_{V1}}{\Omega_{P10}}$
Am-241	59.53	15.148	22.820	31.896	42.334	54.099	67.163	81.501	11.893	17.916	25.042	33.236	42.473	52.730	63.987
Ba-133	80.99	15.323	23.084	32.265	42.823	54.725	67.940	82.444	12.030	18.123	25.331	33.621	42.965	53.340	64.727
Eu-152	121.78	15.558	23.438	32.760	43.480	55.564	68.982	83.709	12.215	18.402	25.720	34.137	43.624	54.159	65.721
Eu-152	244.69	15.969	24.057	33.625	44.628	57.031	70.804	85.919	12.537	18.887	26.399	35.038	44.776	55.588	67.456
Eu-152	344.28	16.174	24.366	34.056	45.201	57.763	71.712	87.022	12.698	19.130	26.738	35.488	45.350	56.302	68.321
Cs-137	661.66	16.573	24.968	34.898	46.317	59.190	73.483	89.171	13.012	19.602	27.398	36.364	46.470	57.692	70.008
Eu-152	778.9	16.674	25.120	35.111	46.600	59.551	73.932	89.716	13.091	19.722	27.566	36.586	46.754	58.045	70.436
Eu-152	964.13	16.808	25.321	35.392	46.973	60.028	74.524	90.433	13.196	19.880	27.786	36.879	47.128	58.509	71.000
Co-60	1173.23	16.931	25.507	35.652	47.319	60.469	75.072	91.098	13.293	20.026	27.991	37.150	47.475	58.939	71.522
Co-60	1332.5	17.012	25.629	35.822	47.544	60.757	75.430	91.533	13.356	20.121	28.124	37.327	47.701	59.220	71.863
Eu-152	1408.01	17.047	25.682	35.896	47.642	60.883	75.585	91.721	13.384	20.163	28.182	37.404	47.799	59.342	72.011
Nuclide	**Energy**	$\frac{\Omega_{V2}}{\Omega_{P4}}$	$\frac{\Omega_{V2}}{\Omega_{P5}}$	$\frac{\Omega_{V2}}{\Omega_{P6}}$	$\frac{\Omega_{V2}}{\Omega_{P7}}$	$\frac{\Omega_{V2}}{\Omega_{P8}}$	$\frac{\Omega_{V2}}{\Omega_{P9}}$	$\frac{\Omega_{V2}}{\Omega_{P10}}$	$\frac{\Omega_{V2}}{\Omega_{P4}}$	$\frac{\Omega_{V2}}{\Omega_{P5}}$	$\frac{\Omega_{V2}}{\Omega_{P6}}$	$\frac{\Omega_{V2}}{\Omega_{P7}}$	$\frac{\Omega_{V2}}{\Omega_{P8}}$	$\frac{\Omega_{V2}}{\Omega_{P9}}$	$\frac{\Omega_{V2}}{\Omega_{P10}}$
Am-241	59.53	13.014	19.605	27.403	36.370	46.477	57.701	70.019	10.308	15.529	21.705	28.808	36.814	45.704	55.462
Ba-133	80.99	13.164	19.832	27.719	36.790	47.015	58.368	70.829	10.427	15.709	21.956	29.141	37.240	46.233	56.103
Eu-152	121.78	13.366	20.136	28.145	37.355	47.736	59.264	71.916	10.587	15.950	22.293	29.588	37.812	46.942	56.964
Eu-152	244.69	13.719	20.668	28.888	38.341	48.997	60.829	73.815	10.867	16.371	22.882	30.370	38.810	48.182	58.468
Eu-152	344.28	13.895	20.933	29.259	38.833	49.625	61.609	74.762	11.006	16.581	23.175	30.759	39.308	48.800	59.218
Cs-137	661.66	14.238	21.450	29.981	39.792	50.851	63.131	76.608	11.278	16.990	23.748	31.519	40.278	50.005	60.681
Eu-152	778.9	14.325	21.581	30.164	40.035	51.162	63.516	77.076	11.347	17.094	23.893	31.711	40.525	50.311	61.051
Eu-152	964.13	14.440	21.754	30.406	40.355	51.571	64.025	77.693	11.438	17.231	24.084	31.965	40.849	50.713	61.540
Co-60	1173.23	14.546	21.914	30.629	40.652	51.950	64.496	78.264	11.522	17.358	24.261	32.200	41.149	51.086	61.992
Co-60	1332.5	14.615	22.018	30.775	40.846	52.198	64.803	78.637	11.577	17.440	24.377	32.354	41.345	51.330	62.288
Eu-152	1408.01	14.645	22.064	30.839	40.930	52.305	64.936	78.799	11.600	17.476	24.427	32.420	41.431	51.435	62.416
Nuclide	**Energy**	$\frac{\Omega_{V3}}{\Omega_{P4}}$	$\frac{\Omega_{V3}}{\Omega_{P5}}$	$\frac{\Omega_{V3}}{\Omega_{P6}}$	$\frac{\Omega_{V3}}{\Omega_{P7}}$	$\frac{\Omega_{V3}}{\Omega_{P8}}$	$\frac{\Omega_{V3}}{\Omega_{P9}}$	$\frac{\Omega_{V3}}{\Omega_{P10}}$	$\frac{\Omega_{V3}}{\Omega_{P4}}$	$\frac{\Omega_{V3}}{\Omega_{P5}}$	$\frac{\Omega_{V3}}{\Omega_{P6}}$	$\frac{\Omega_{V3}}{\Omega_{P7}}$	$\frac{\Omega_{V3}}{\Omega_{P8}}$	$\frac{\Omega_{V3}}{\Omega_{P9}}$	$\frac{\Omega_{V3}}{\Omega_{P10}}$
Am-241	59.53	11.180	16.843	23.542	31.246	39.930	49.572	60.155	8.935	13.460	18.813	24.970	31.909	39.615	48.072
Ba-133	80.99	11.310	17.038	23.814	31.607	40.391	50.145	60.850	9.038	13.616	19.031	25.258	32.278	40.073	48.628
Eu-152	121.78	11.483	17.300	24.180	32.092	41.011	50.915	61.784	9.177	13.825	19.323	25.646	32.774	40.688	49.374
Eu-152	244.69	11.786	17.756	24.818	32.939	42.094	52.259	63.415	9.419	14.190	19.833	26.323	33.639	41.762	50.678
Eu-152	344.28	11.937	17.984	25.137	33.362	42.634	52.930	64.229	9.540	14.372	20.088	26.661	34.070	42.298	51.328
Cs-137	661.66	12.232	18.428	25.757	34.186	43.687	54.237	65.815	9.775	14.727	20.584	27.319	34.912	43.343	52.595
Eu-152	778.9	12.307	18.541	25.915	34.395	43.954	54.568	66.218	9.835	14.817	20.709	27.486	35.125	43.607	52.917
Eu-152	964.13	12.405	18.689	26.122	34.670	44.305	55.005	66.747	9.914	14.935	20.875	27.706	35.406	43.956	53.340
Co-60	1173.23	12.497	18.827	26.314	34.925	44.631	55.409	67.238	9.987	15.045	21.029	27.910	35.667	44.280	53.733
Co-60	1332.5	12.556	18.916	26.440	35.092	44.844	55.673	67.559	10.034	15.117	21.129	28.043	35.837	44.491	53.989
Eu-152	1408.01	12.582	18.955	26.494	35.164	44.936	55.788	67.698	10.055	15.148	21.172	28.101	35.910	44.582	54.100

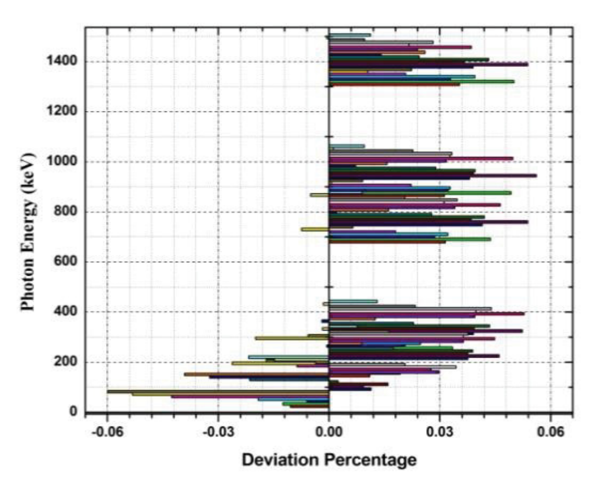

Figure 4a: The deviation between the calculated effective solid angle ratio, R, that obtained empirically and the experimental one for D1.

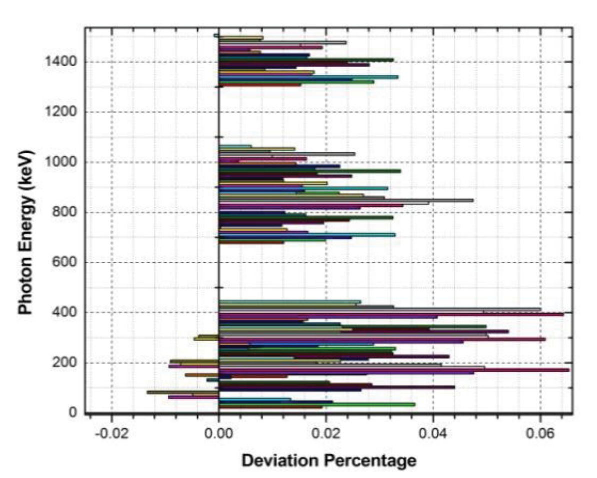

Figure 4b: The deviation between the calculated effective solid angle ratio, R, that obtained empirically and the experimental one for D2.

REFERENCES

1. Debertin K, Helmer RG. Gamma- and X-ray spectrometry with semiconductor detectors. North-Holland. 1988; New York. Ref.: https://goo.gl/fHfUb8

2. Lippert J. Detector-efficiency calculation based on point-source measurement. Int J Appl Radiat Isot. 1983; 34: 1097-1103. Ref.: https://goo.gl/wOQveD

3. Moens L, Hoste J. Calculation of the peak efficiency of high-purity germanium detectors. Int J Appl Radiat Isot. 1983; 34: 1085-1095. Ref.: https://goo.gl/j3IxZv

4. Haase G, Tait D, Wiechon A. Application of new monte carl method for determination of summation and self-attenuation corrections in gamma spectrometry. Nucl Instrum Methods. 1993; A336: 206-214. Ref.: https://goo.gl/x4tnng

5. Wang TK, Mar WY, Ying TH, Liao CH, Tseng CL, et al. HPGe detector absolute-peak-efficiency calibration by using the ESOLAN program. Appl Radiat Isot. 1995; 46: 933-944. Ref.: https://goo.gl/Lgl3lc

6. Wang TK, Mar WY, Ying TH, Tseng CH, Liao CH, et al. HPGe Detector efficiency calibration for extended cylinder and Marinelli- beaker sources using the ESOLAN program. Appl Radiat Isot. 1997; 48: 83-95. Ref.: https://goo.gl/dQNx77

7. Lépy MC, Altzitzoglou T, Arnold D, Bronson F, Capote Noye R, et al. Intercomparison of efficiency transfer software for gamma-ray spectrometry. Appl Radiat Isot. 2001; 55: 493-503. Ref.: https://goo.gl/WfSS3v

8. Vidmar T, Aubineau Laniece I, Anagnostakis MJ, et al. An intercomparison of monte carlo codes used in gamma-ray spectrometry. Appl Radiat Isot. 2008; 66: 764-768. Ref.: https://goo.gl/e35Sd8

9. Badawi MS, El-Khatib AM, Krar ME. New numerical simulation approach to calibrate the NaI(Tl) detectors array using non-axial extended spherical sources. Journal of Instrumentation. 2013; 8: 11. Ref.: https://goo.gl/ut1p4i

10. Badawi MS, Krar ME, El-Khatib AM, Jovanovic SI, Dlabac AD, et al. A new mathematical model for determining the full energy peak efficiency (FEPE) for an array of two γ-detectors counting rectangular parallelepiped source. Nuclear Technology & Radiation Protection Journal. 2013; 28: 370-380. Ref.: https://goo.gl/LYmnac

11. Badawi MS, Elzaher MA, Thabet AA, El-khatib AM. An empirical formula to calculate the full energy peak efficiency of scintillation detectors. Appl Radiat Isot. 2013; 74: 46-49. Ref.: https://goo.gl/V5PDsr

12. Abbas MI. A direct mathematical method to calculate the efficiencies of a parallelepiped detector for an arbitrarily positioned point source. Radiat Phys Chem. 2001a; 60: 3-9. Ref.: https://goo.gl/JypVh5

13. Abbas MI. Analytical formulae for well-type NaI(Tl) and HPGe detectors efficiency computation. Appl Radiat Isot. 2001b; 55: 245-252. Ref.: https://goo.gl/hLQSKd

14. Abbas MI, SelimYS. Calculation of relative full-energy peak efficiencies of well-type detectors. Nucl Instrum Methods A. 2002; 480: 651-657. Ref.: https://goo.gl/9AMrXx

15. Abbas MI. HPGe detector absolute full-energy peak efficiency calibration including coincidence correction for circular disc sources. J Phys D Appl Phys. 2006; 39: 3952-3958. Ref.: https://goo.gl/89DOYb

16. Abbas MI, Nafee SS, Selim YS. Calibration of cylindrical detectors using a simplified theoretical approach. Appl Radiat Isot. 2006; 64: 1057-1064. Ref.: https://goo.gl/M4DM6l

17. Debertin K, Schotzig U. Coincidence summing corrections in Ge(Li)-spectrometry at low source-to-detector distances. Nucl Instrum Meth A. 1979; 158: 471-477. Ref.: https://goo.gl/CJ5NGn

18. El-Khatib AM, Thabet AA, Elzaher MA, Badawi MS, Salem BA. Study on the effect of the, self-attenuation coefficient on γ-ray detector efficiency calculated at low and high energy regions. Journal of Nuclear Engineering and Technology. 2014; 46: 217-224. Ref.: https://goo.gl/wpoBxl

19. El-Khatib AM, Badawi MS, Elzaher MA, Thabet AA. Calculation of the peak efficiency for NaI(Tl) gamma ray detector using the effective solid angle method. Journal of Advanced Research in Physics. 2012; 3: 021204. Ref.: https://goo.gl/bqKYOW